Structural insights into allosteric modulation of mGlu2

Metabotropic glutamate receptors (mGlus) belong to the class C G-protein-coupled receptor (GPCR) family and are involved in brain physiological functions as well as neuropathological processes. In response to glutamate, one of the major excitatory neurotransmitters, mGlu2 plays important roles in modulating cell excitability and synaptic transmission and displays potential as a drug target for the treatment of glutamate-related neuropsychiatric diseases such as depression and schizophrenia [1]. This receptor contains a large extracellular domain (ECD) composed of the Venus flytrap (VFT) domain that binds agonist and a cysteine-rich domain (CRD) connected to a seven-helical transmembrane domain (TMD) responsible for G protein coupling. Because of the highly conserved orthosteric binding pocket of mGlu receptors in ECD, the allosteric pocket in the TMD of mGlu receptors is believed to be a better site for the designation of mGlu-selective drugs (Fig. 1) [2]. However, the lack of high-resolution structural details of the mGlu2 allosteric site and the poor understanding of the allosteric modulating mechanism have hindered the development of highly selective mGlu2 negative allosteric modulators (NAMs) and positive allosteric modulators (PAMs). Here, we solved two crystal structures of the mGlu2 TMD bound to two NAMs (NAM563 and NAM597), which provided high-resolution molecular details of the NAM-binding modes of mGlu2.

To facilitate the crystallization of the mGlu2 TMD-NAM complex, the extracellular domain (residues 1 to 555) and C-terminus (residues 846 to 872) of mGlu2 were removed and a fusion protein, flavodoxin, was inserted in intracellular loop 2 to reduce the receptor flexibility. Two point mutations, $N655^{3.52}Y$ and $H815^{7.53}Y$, were further introduced to improve the receptor stability without affecting the ligand binding. The crystals of mGlu2-TMD with NAM563 and NAM597 were optimized using the lipidic cubic phase (LCP), and diffraction data were collected at SPring-8 **BL41XU**. The structures of NAM563- and NAM597-bound mGlu2 TMDs were determined by molecular replacement at final resolutions of 2.5 Å and 2.7 Å, respectively.

The overall fold of the mGlu2 TMD structure consists of a canonical seven-transmembrane (7TM) bundle of α-helices. The binding pockets of NAM563 and NAM597 are formed by helices III, V, VI, and VII of the transmembrane regions in mGlu2, which is similar to the previously reported NAM-binding pockets of mGlu1 and mGlu5 [3]. The main skeletons of these two NAMs share similar interaction patterns with mGlu2 but are different on the extracellular side (Fig. 2). Mutations of some residues within the

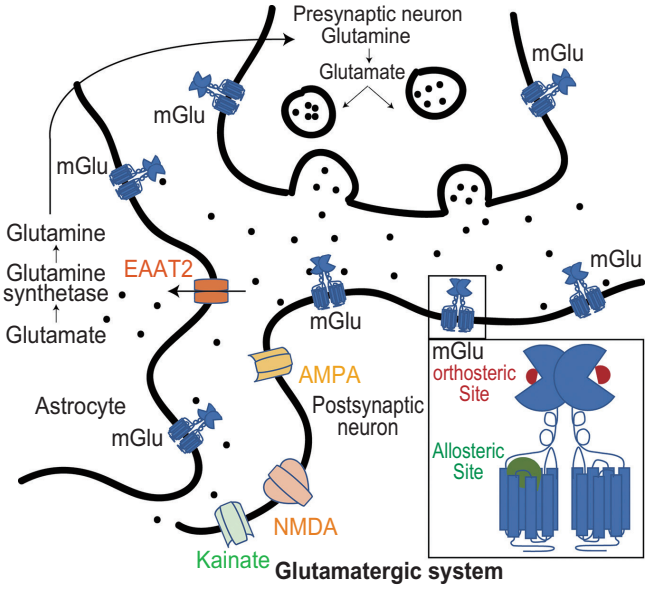

Fig. 1. Diagram of the glutamatergic system in neurons and allosteric regulation of mGlu receptors. (EAAT2: excitatory amino acid transporter-2, AMPA: α-amino-3-hydroxy-5-methyl-4-isoxazole-propionic acid receptor, NMDA: N-methyl-D-aspartic acid receptor, and Kainate: Kainate receptor)

binding pockets exhibit a 5- to 1000-fold reduction in the inhibitory activity of these two NAMs, whereas other residues display a variety of effects on NAM binding, suggesting that different NAMs may occupy similar binding cavities in mGlu2 but adopt distinct interaction patterns when binding to the receptor [3]. A detailed analysis of the NAM563-bound mGlu2 TMD and our recently solved mGlu2 in complex with PAM JNJ-40411813 structures disclosed a rotamer conformational change of the highly conserved residue W773$^{6.50}$ in class C GPCRs [4] (Fig. 3(a)). This conformational change disrupts the interaction core in the transmembrane helical bundle and releases it from the constraint of the inactive state, which potentially leads to the downward movement of helix VI. The conformational change of helix VI may further lead to the alteration of the intracellular interaction network of mGlu2 and is associated with receptor activation. Besides the typical ionic lock of class C GPCRs between the highly conserved residues K$^{3.50}$ and E$^{6.35}$, additional ionic interaction formed by R656$^{3.53}$ in helix III and E754 in the intracellular loop (ICL) 3 was observed in the mGlu2 TMD-NAM563 structure (Fig. 3(b)). However, these interactions are broken in the PAM bound structure, which is probably attributable to the downward movement of helix VI and the rearrangement of ICL3.

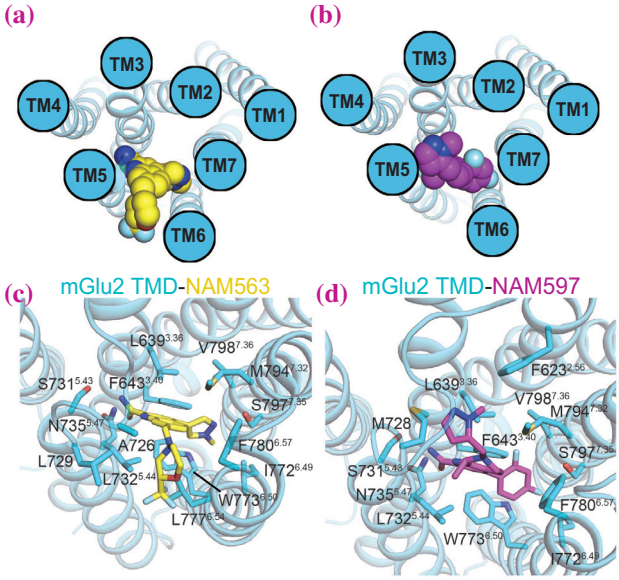

Fig. 2. Crystal structures of NAM-bound mGlu2 TMD showing the different binding patterns of NAMs. The trifluoromethyl-morpholin group of NAM563 squeezes into a gap between helices VI and VII, whereas the methyl-pyrazol group in NAM597 points to the opposite direction to interact with helix II and ECL2. **(a)** NAM563 and **(b)** NAM597 in mGlu2 TMD. **(c)** NAM563- and **(d)** NAM597-binding pocket and ligand receptor interactions.

These studies reveal the molecular details of interaction modes for two NAMs with mGlu2 TMD and explain the negative allosteric modulation mechanisms of mGlu2. Together with the recently solved PAM-bound mGlu2 structure, these structures offer direct models for the development of mGlu2 specific modulators.

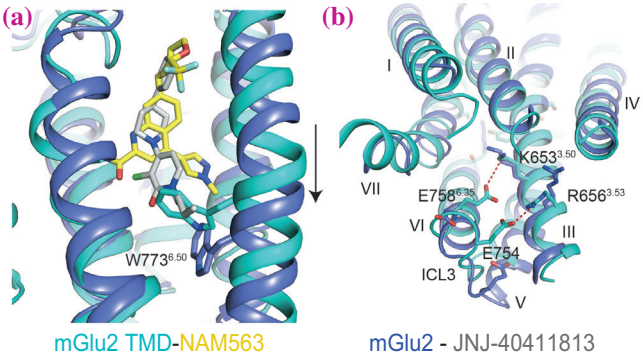

Fig. 3. Conformational change between NAM-bound mGlu2 and PAM-bound mGlu2-G_{i1} complexes. **(a)** Conformational change of W$^{6.50}$ and helix VI upon activation. In the NAM563-bound mGlu2 TMD structure, NAM563 constrains the conformation of its side chain to stabilize the receptor in the inactive state. In the JNJ-40411813-bound structure, the side chain of W773$^{6.50}$ exhibits downward rotation by approximately 90°. NAM563, PAM JNJ-40411813, and corresponding receptors are shown as yellow/gray sticks and cyan/purple cartoons. The black arrow indicates the downward shift of helix VI upon PAM binding. **(b)** Ionic locks of NAM-bound mGlu2 and PAM-bound mGlu2-G_{i1} complex. The ionic interactions are shown as red dashed lines.

S. Lin, J. Du, B. Wu* and Q. Zhao

Shanghai Institute of Materia Medica,
Chinese Academy of Sciences

*Email: beiliwu@simm.ac.cn

References

[1] S. Chaki: Adv Pharmacol. **86** (2019) 97.
[2] Z. Orgován *et al.*: Curr Top Med Chem. **19** (2019) 1768.
[3] *J. Du, D. Wang, H. Fan, C. Xu, L. Tai, S. Lin, S. Han, Q. Tan, X. Wang, T. Xu, H. Zhang, X. Chu, C. Yi, P. Liu, X. Wang, Y. Zhou, J.-P. Pin, P. Rondard, H. Liu, J. Liu, F. Sun, B. Wu and Q. Zhao: Nature* ***594*** *(2021) 589.*
[4] S. Lin *et al.*: Nature **594** (2021) 583.